mathematics

Article

Dynamics and Global Bifurcations in Two Symmetrically Coupled Non-Invertible Maps

Yamina Soula [1], Hadi Jahanshahi [2,*], Abdullah A. Al-Barakati [3] and Irene Moroz [4]

1 Department of Mathematics, University of Oum el Bouaghi, Oum El Bouaghi 04000, Algeria
2 Department of Mechanical Engineering, University of Manitoba, Winnipeg, MB R3T 5V6, Canada
3 Communication Systems and Networks Research Group, Department of Information Systems, Faculty of Computing and Information Technology, King Abdulaziz University, Jeddah 21589, Saudi Arabia
4 Mathematical Institute, University of Oxford, Oxford OX2 6GG, UK
* Correspondence: jahanshahi.hadi@ieee.org

Abstract: The theory of critical curves determines the main characteristics of a discrete dynamical system in two dimensions. One important property that has garnered recent attention is the problem of chaos synchronization, along with the location of its chaotic attractors, basin boundaries, and bifurcation mechanisms. Varying the parameters of the maps reveals the instrumental role that these curves play, where the bifurcation leads to complex topological structures of the basins occurs by contact with the basin boundaries, resulting in the appearance or disappearance of some components of the basin. This study focuses on the properties of a discrete dynamical system consisting of two symmetrically coupled non-invertible maps, specifically those with an invariant one-dimensional submanifold (or one-dimensional maps). These maps exhibit a complex structure of basins with the coexistence of symmetric chaotic attractors, riddled basins, blow-out, on-off intermittency, and, most significantly, the appearance of chaotic synchronization with a correlation between all the characteristics. The numerical method of critical curves can be used to demonstrate a wide range of dynamic scenarios and explain the bifurcations that lead to their occurrence. These curves play a crucial role in a system of two symmetrically coupled maps, and their significance will be discussed.

Keywords: coupled non-invertible maps; symmetry; contact bifurcations; critical curves; basins of attraction

MSC: 34D06; 37D45; 35B32; 32S50

check for updates

Citation: Soula, Y.; Jahanshahi, H.; Al-Barakati, A.A.; Moroz, I. Dynamics and Global Bifurcations in Two Symmetrically Coupled Non-Invertible Maps. *Mathematics* **2023**, *11*, 1517. https://doi.org/10.3390/math11061517

Academic Editor: Higinio Ramos

Received: 15 February 2023
Revised: 17 March 2023
Accepted: 17 March 2023
Published: 21 March 2023

1. Introduction

In 1996, Ding and Yang presented an instance of a map that has intertwined basins. This map is defined as a coupled map on the interval $[-1,1]^2$, with $T(x,y) = (x', y')$ as its expression.

$$\begin{cases} x' = f_a(x) + b[f_a(y) - f_a(x) + f_a(y)^3 - f_a(x)^3], \\ y' = f_a(y) + b[f_a(x) - f_a(y) + f_a(x)^3 - f_a(y)^3], \end{cases} \tag{1}$$

The function $f_a(x) = ax(1-x^2)\exp(-x^2)$ with $a = 3.4$ and $b = 0.48$ defines a map that has attractors A on both sides of the origin along the diagonal $x = y$. The map $f_a(x)$ has two chaotic attractors for $a = 3.4$, namely A^+ in the region $x > 0$ and A^- in the region $x < 0$. According to [1], for $b_1 \leq b \leq b_2$, the attractors $A^{\pm}$ are global attractors, where $b_1 = 0.4701$ and $b_2 = 0.594$ are two transition parameters. The authors of [1] provide evidence to support their claim that the basins of attraction in the interval $[b_1, b_2]$ are intermingled, and that $A^{\pm}$ are Milnor attractors [2].

In this study, we introduce a new model that is a modification of the model described in [1]. The new model is defined by the following system of equations:

$T(x,y) = (x^{'}, y^{'}), \quad (x,y) \in \mathbb{R}^2$

$$T : \begin{cases} x^{'} = f_a(x) + b(y - x), \\ y^{'} = f_a(y) + b(x - y), \end{cases} \tag{2}$$

The behavior of the map T is simplified to a one-dimensional map f_a when restricted to the diagonal $\Delta = (x, x) \in \mathbb{R}^2$, which was also observed in [1].

$$f_a : x \to ax(1 - x^2)\exp(-x^2), \tag{3}$$

In this context, $a \in \mathbb{R}^*$ and $b \in \mathbb{R}$ represent the coupling parameter for the symmetric dynamical system. If the trajectory of the system is bounded and $\|y_n - x_n\| \to 0$ as $n \to \infty$, where $x = y$ is the synchronization subspace of the one-dimensional restriction of T to Δ, then the trajectory synchronizes [3]. The chaotic set in the invariant subspace attracts a set of positive Lebesgue measure points [4,5].

In 1992, Alexander et al. [3] provided a precise definition of a riddled basin. Note that the basin of attraction $B(A)$ can only be riddled if $B(A)$ has a positive measure, i.e., if A is a Milnor attractor. Riddled basins of attraction and intermingled basins can be observed on the other side of the blow-out bifurcation, where the transverse Lyapunov exponent $\Lambda_\perp$ changes sign [6,7].

An asymptotically stable attractor is referred to as a topological attractor, while a closed invariant set is a weak attractor in the Milnor sense, or simply a Milnor attractor, if its stable basin has positive Lebesgue measure.

Critical sets play an important role in chaotic synchronization problems, particularly in chaotic dynamical systems that have fixed submanifolds with dimensions less than that of the total phase space. Milnor attractors, which are unstable in the Lyapunov sense, occur naturally, along with new phenomena such as on-off intermittency and riddled basins (as well as riddling and blowout bifurcations) [8–11].

When the iterated map is non-invertible, as is often the case in chaos synchronization situations, the technique of critical sets can be used to illustrate the global fate of locally repelled trajectories following a riddling bifurcation [12]. Consequently, the basin of attraction of an attractor within an invariant manifold might be riddled with a positive measure set of points belonging to the basins of other attractors [13,14]. The critical sets method is a powerful tool for describing global dynamical properties [15–17]. The state space is repeatedly folded when a non-invertible map is iteratively applied, which typically allows one to create a restricted region where asymptotic dynamics are trapped [18,19]. On the other hand, the iterative application of the inverse repeatedly unfolds the state space, allowing a neighborhood of an attractor to have pre-images far away. This can result in complex topological basin structures, which may be constructed by the union of numerous disconnected parts. If a parameter change causes a crossing between a basin boundary and a critical set, causing a piece of the basin to enter an area with a higher number of inverses, new basin components arise after the contact [20,21].

This article aims to elucidate the global dynamic characteristics of a symmetrical system represented by a non-invertible 2D map (2) that remains unchanged on the diagonal of the phase plane. This map exhibits a highly intricate basin structure with the coexistence of symmetric chaotic attractors, riddled basins, blow-out, on-off intermittency, and most notably, chaotic synchronization with correlations between all the characteristics. The instrumental role of critical curves in describing these complex dynamic properties is discussed in this paper, utilizing the numerical method of critical curves [7,22] and software such as Fortran and Matlab to analyze and solve technical and scientific issues.

Critical curves are essential singularities utilized to study basin bifurcations [23–25]. These singularities are fundamental in the structure of attractors and basins, as well as their bifurcations. Contact bifurcations, which occur at the boundary between the basins of attraction and critical sets, are a prime example of such bifurcations, leading to global bifurcations [26–29].

The paper is organized as follows. The stability domains for the coupled maps (2) are presented in Section 2. Section 3 discusses some generic features of non-invertible maps and contact bifurcations using critical curves. Section 4 summarizes the research on chaotic synchronization, riddling, and on-off intermittency.

2. Stability Domains of Map (2) in the Parameter Space

The stability regions for the coupled map (2) can be numerically constructed in parameter space, revealing the diversity of coexisting attractors [30–37]. In a specific region of the real parameter (a, b) plane, a family of bifurcations is identified, where the mappings exhibit simple dynamics. The first few bifurcation curves in this family are computed, and the resulting bifurcation diagram, consisting of these bifurcation curves in the parameter (a, b) plane along with sample phase portraits, is studied. Figure 1 presents information on the stability region for fixed points (blue domain) and the existence region for attracting cycles of period k (up to $k = 10$), as well as the regions where bounded iterated sequences exist (black regions, $k = 11$), and the no-admissible region (white region, no cycles zone). The bifurcation structure is of a complex type, with Mira [18] indicating that the bifurcation curve is the line separating two regions of different colors.

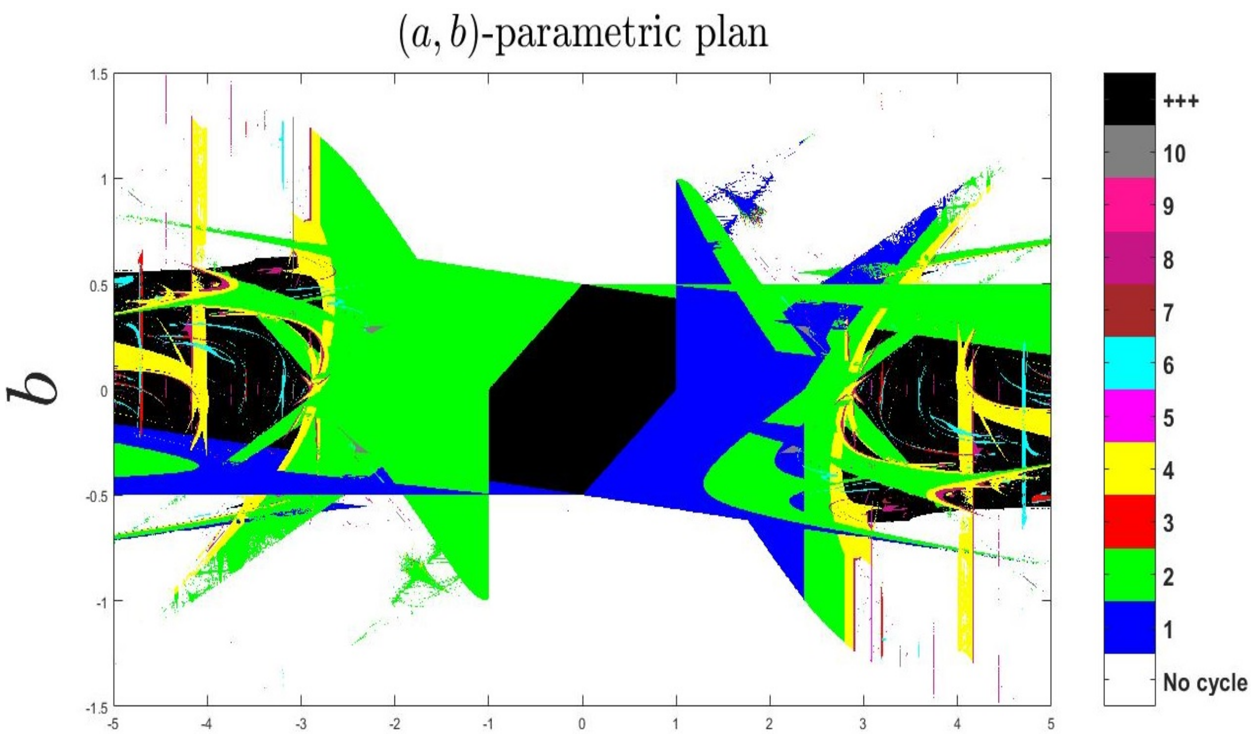

Figure 1. Stability domains for the coupled map (2) in the parameter space (a, b).

3. Properties of Non-Invertible Map (2) in the Phase Space

3.1. Critical Sets

The geometric properties of two-dimensional maps provide an intuitive visualization of the relationship between the locus of points where the Jacobian determinant ($\det DT(x, y)$) vanishes and the folding properties of two-dimensional non-invertible maps. In fact, while invertible maps are usually characterized by the fact that the sign of $\det DT(x, y)$ does not change in the entire phase plane, critical sets of a two-dimensional non-invertible map are an important mathematical tool used to study basin bifurcations. They were introduced in 1964 by Mira [18] and the critical curve LC (French notation, i.e., Ligne Critique) is defined as the locus of points having at least two coincident rank-1 pre-images, located on the set of merging pre-images denoted by LC_{-1}, i.e., $LC = T(LC_{-1})$.

For a continuously differentiable map T, the set LC_{-1} is included in the set of points in which the Jacobian determinant of T equals zero and changes its sign.

Global bifurcations, which give birth to complicated topological structures of basins, can be explained in terms of connections between basin boundaries and critical sets. If there are any locations in phase space where the map does not contain a unique rank-one pre-image, the state space is partitioned into Z_k zones (characterized by a variable number k of inverses ($k \geq 0$)). Because the critical curves LC separate these regions, the number of first rank pre-images changes only when the LC is crossed, with the exception of singular points.

Note that critical sets LC of rank k ($k \geq 1$) are the image of the LC_{-1} rank k and are represented by:

$$LC_{k-1} = T^{k}(LC_{-1}) = T^{k-1}(LC), \quad LC_0 = LC.$$

The map T defined by (2) is continuous and differentiable in the whole of $\mathbb{R}^2$. The critical set LC_{-1} is a subset of the locus of points where the determinant of the Jacobian matrix of T is zero.

The Jacobian matrix of T is given by $DT(x,y)$ and can be computed as:

$$DT(x,y) = \begin{bmatrix} g(x) - b & b \\ b & g(y) - b \end{bmatrix}.$$

With:

$$g(x) = a\exp(-x^2)(1 - 5x^2 + 2x^4),$$

LC_{-1} is constructed by points $(x,y) \in \mathbb{R}^2$, which satisfy the following equation:

$$\begin{aligned}
&4a^2e^{-x^2-y^2}x^4y^4 + (2a^2e^{-x^2-y^2} - 10a^2e^{-x^2-y^2}y^2 - 2ae^{-x^2}b)x^4 + \\
&(2a^2e^{-x^2-y^2} - 10a^2x^2e^{-x^2-y^2} - 2bae^{-y^2})y^4 + (25a^2e^{-x^2-y^2})x^2y^2 + \\
&(-5a^2e^{-x^2-y^2} + 5abe^{-x^2})x^2 + (-5a^2e^{-x^2-y^2} + 5bae^{-y^2})y^2 + \\
&a^2e^{-x^2-y^2} - bae^{-x^2} - bae^{-y^2} = 0.
\end{aligned}$$

The equation for LC_{-1} depends on both parameters a and b. In the (x,y) phase plane, LC_{-1} is formed by five disjoint branches, namely:

$$LC_{-1} = \bigcup_{i=1}^{5} LC_{-1}^{(i)}$$

Additionally, as either the parameter a or b varies, the equation for the curves that make up the critical set of rank-1, $LC = T(LC_{-1})$, shift (as shown in Figure 2), and it is formed by nine non-disjoint branches:

$$LC = \bigcup_{i=1}^{9} LC^{(i)}.$$

A crossing between a basin boundary and a critical set LC_{-1} and LC, which separates different zones Z_k, is caused by a parameter variation. The branches of the critical sets LC_{-1} and LC move in the (x,y) phase plane as the parameter a or b varies (see Figure 2). The black lines represent the branches of the critical set of rank-1 LC_{-1}, and the red lines represent the branches of the critical set of rank-k LC.

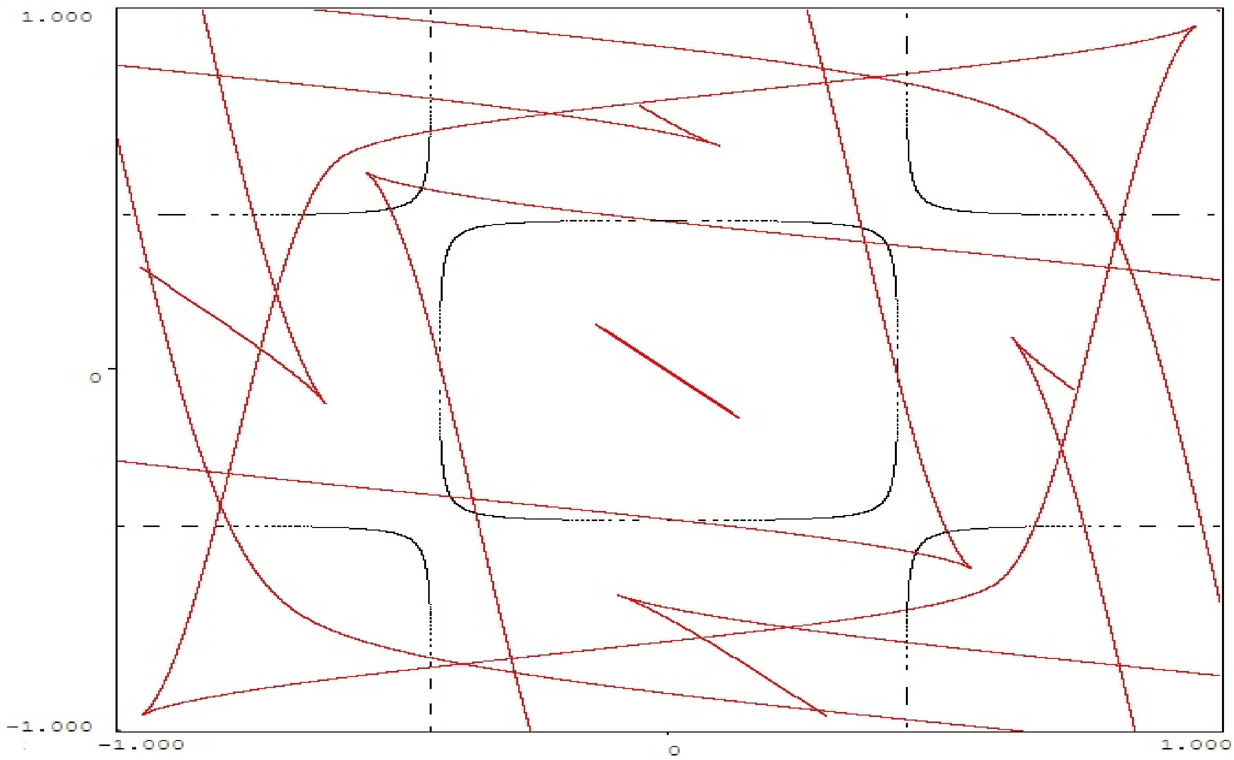

Figure 2. The branches of LC_{-1} (black lines) and LC (red lines) for map (2) with $a = 3.4$ and $b = 0.48$.

3.2. Basins of Attraction

Depending on the relation between the basin boundaries and the critical set LC, the basins created by two-dimensional non-invertible maps may exhibit a range of topological structures, including simply connected, multiply connected, or disconnected basins [38,39].

To understand the emergence of the complex basin structures, we will explore several global bifurcations that signal the transition to the rising complexity of the basins.

The basins of attraction of the non-invertible map T described by Equation (2) often exhibit complex topological features, such as sets with fractal boundaries or disconnected sets.

The goal of this paper is to investigate the evolution of the basins of attraction as the control parameter a is varied in the map 2, using the terminology of [18]. Specifically, we will study how the basins become fractal, unconnected, simply connected, or multiply connected.

To achieve this, we will use the classical bifurcations that are directly related to those experienced by the boundary ∂B of a domain (basin) B. These bifurcations, also known as global or contact bifurcations, characterize the path to basin boundaries as the control parameter a is varied. One such bifurcation, well known in the literature [15], occurs due to contacts between critical curves and basin boundaries.

We give the following codes:

- $B(E_k)$: Basin of attraction of period k, $(k = 1, 2, 3, ..., 14)$.
- The black regions is the basin of attraction of period k ($k \geq 15$).
- $B(A)$: Basin of attraction of a chaotic attractor A (white color).
- We have the fixed point $(0, 0) \in \Delta \cap \Delta_{-1}$, where $\Delta = \{(x, y) \setminus y = x\}$, and the antidiagonal $\Delta_{-1} = \{(x, y) \setminus y = -x\}$.

We begin by considering a scenario where the green basin of period 2, $B(E_2)$, has a fractal shape (shown in green in Figure 3) at $a = 3.4$, while the white basin of chaotic attractors, $B(A)$, contains chaotic attractors A_1 and A_2 that are created by the evolution of Neimark bifurcations. One of the Neimark bifurcations occurs in the region $(x, y) \in [-1, 0] \times [0, 1]$, denoted as A_1, and the other in the region $(x, y) \in [0, 1] \times [-1, 0]$, denoted as A_2 (see Figure 3, at $a = 3.6$). The chaotic attractors A_1 and A_2 are symmetrical with respect to the diagonal Δ.

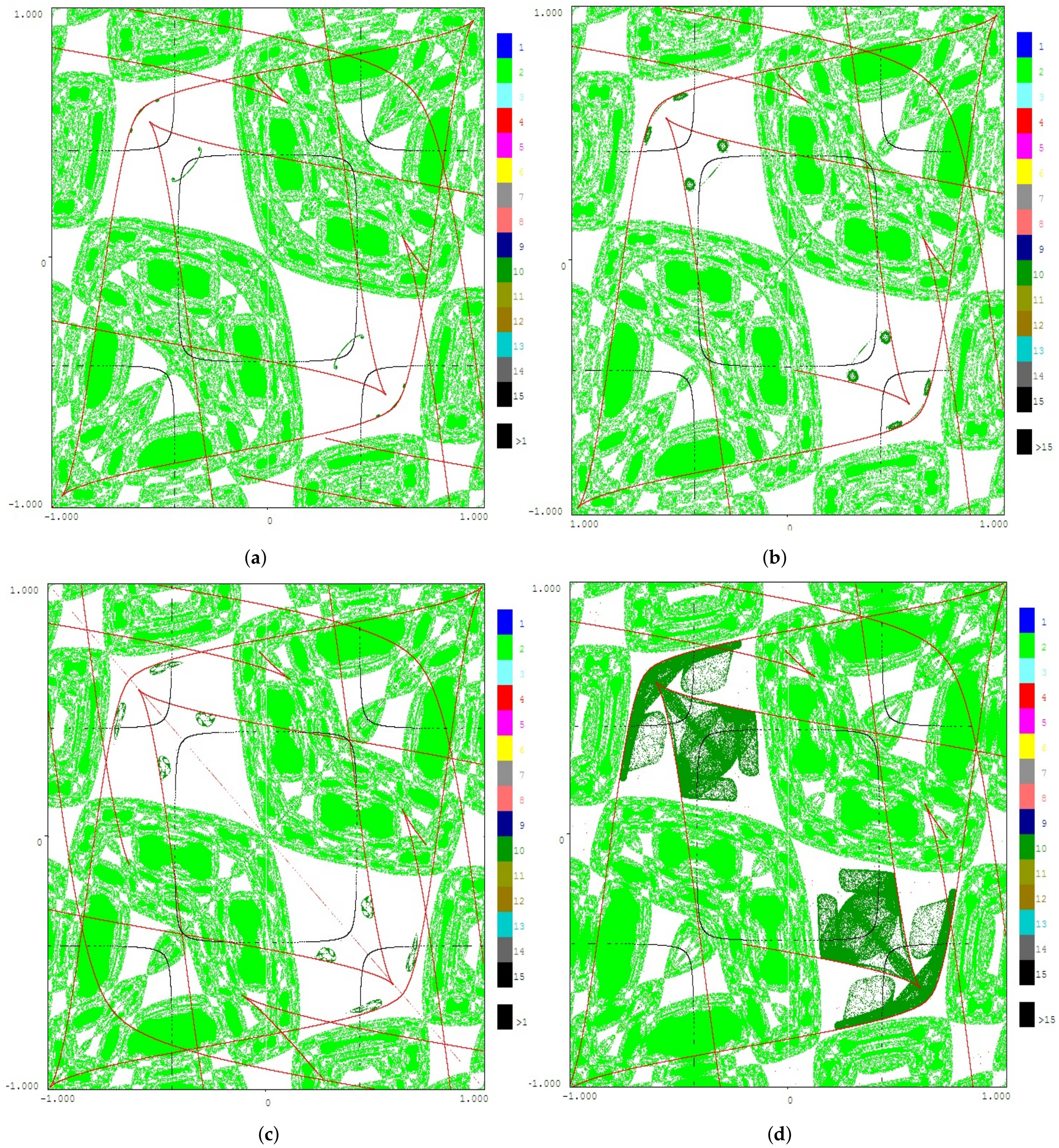

Figure 3. For: (**a**) $a = 3.4$, (**b**) $a = 3.45$, (**c**) $a = 3.52$, (**d**) $a = 3.6$, and $b = 0.48$, green color basin of a period 2, $B(A)$: basin of chaotic attractor (white color), $B(E_2)$ and $B(A)$ are sets that are not connected. Black lines and red lines correspond to LC_{-1} and LC, respectively.

At $a = 3.626$ (shown in Figure 4), the basin of attraction $B(A)$ (white color) exhibits a mixed structure between the basins of period 6 and 12 (flip bifurcations). After the contact bifurcation between the boundary of basins with a portion of the LC, the basin structure is not fractally connected, and it is formed by many separate parts. These bifurcations lead to a fractalization of the total basins. At $a = 3.9$, $B(A_j)$, $j = 1, 2$ disappear.

The $B(E_2)$ basin becomes simply connected, i.e., we have the bifurcation "$B(E_2)$ and the unconnected $\leftrightarrow B(E_2)$ becomes simply connected", with the existence of one synchronized and one antisynchronized chaotic attractors along the diagonal Δ and the antidiagonal Δ_{-1}, respectively.

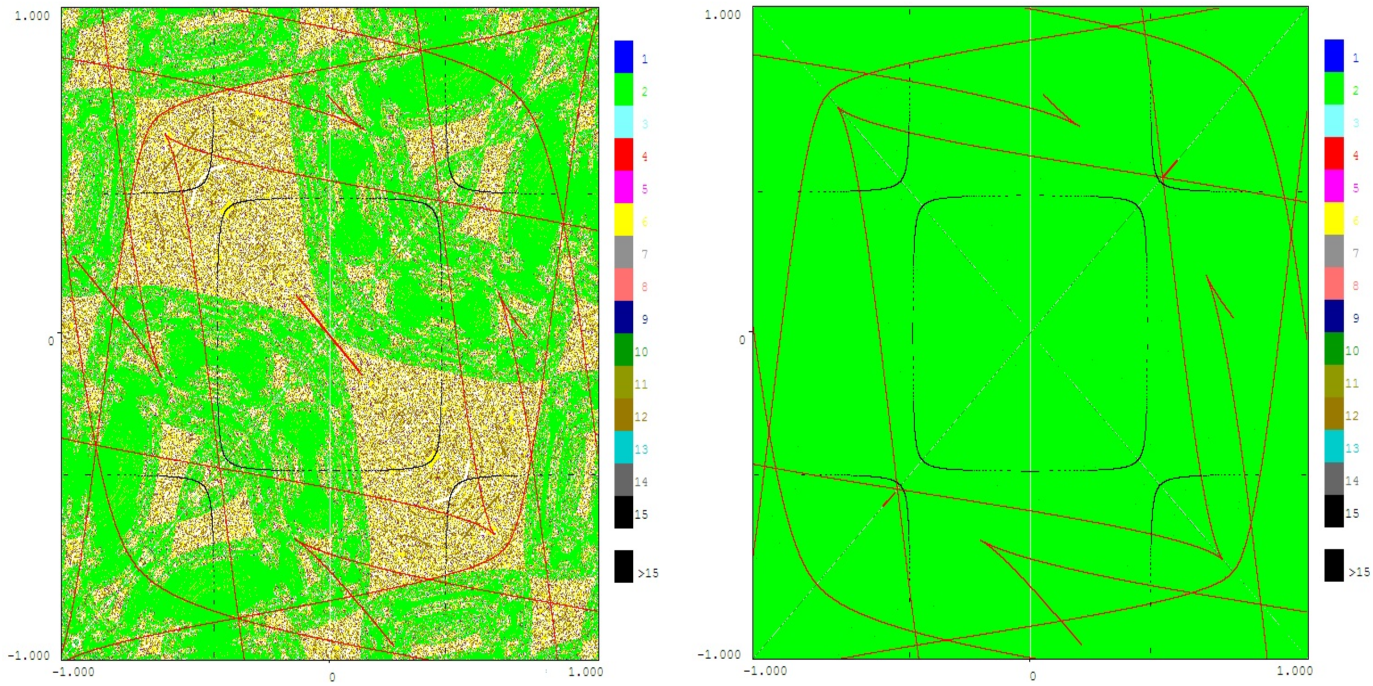

(**a**) (**b**)

Figure 4. For $b = 0.48$ and (**a**) $a = 3.626$, the basin of attraction $B(A)$ (white color) shows a mixed structure between the basins of period 6 and 12. After the contact bifurcation between LC and the boundary of basin, these bifurcations causes a phenomenon fractalization of the total basins (non-connected basins with a fractal structure). At (**b**) $a = 3.9$, the disappearance of $B(A)$, the $B(E_2)$ became simply connected basin, i.e., we have the bifurcation "$B(E_2)$ non-connected $\leftrightarrow B(E_2)$ simply connected" with the existence of one synchronized and one antisynchronized chaotic attractors along the diagonal Δ and the antidiagonal Δ_{-1}, respectively.

Specifically, we choose x from the interval $[-0.924, -0.084]$ and y from the interval $[0.074, 0.534]$, with $b = 0.6$ and vary a (see Figure 5) Here, we provide additional numerical details for Figure 6.

When $a = 4$, there is a tangency or contact between the unconnected basin boundary and the branches of LC (see Figure 5). The result of the sequence of bifurcations at $a = 4.01$ and $a = 4.03$ is that the basins become smaller and smaller. At the next bifurcation, $a = 4.09$, we observe the disappearance of the basin $B(A)$ (white color) and the appearance of $B(E_6)$ (yellow color). At $a = 4.11$, the basin $B(E_6)$ disappears, and the appearance of $B(E_{12})$ (brown color) is the result of a flip (period doubling) bifurcation.

After the contact bifurcations between the boundaries of the basins and particular portions of LC, we observe the following type of bifurcation:

"$B(E_1)$ unconnected $\longleftrightarrow B(E_1)$ simply connected" at $a = 4.22$, which is the final bifurcation.

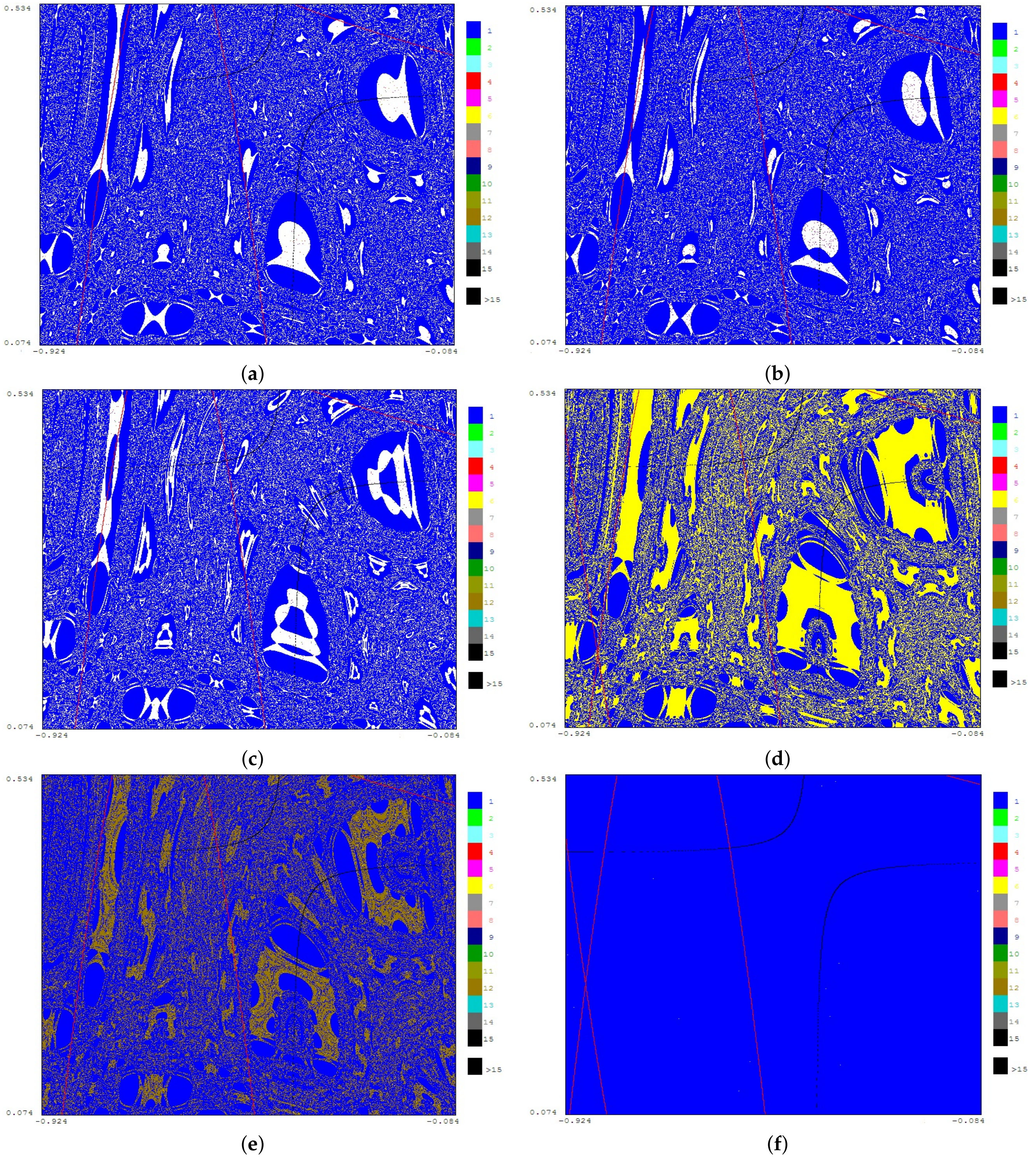

Figure 5. Details of Figure 6, changes of the connectivity of the basins after the contact bifurcation between LC and the basin boundary; this contact will mark a bifurcation "$B(E_1)$ no-connected $\longleftrightarrow$ $B(E_1)$ simply connected" for $b = 0.6$, a small increase of (**a**) $a = 4$, (**b**) $a = 4.01$, (**c**) $a = 4.03$, (**d**) $a = 4.09$, (**e**) $a = 4.11$, and (**f**) $a = 4.22$ are shown when (x, y) are in the regions: $[-0.924, -0.084] \times [0.074, 0.534]$.

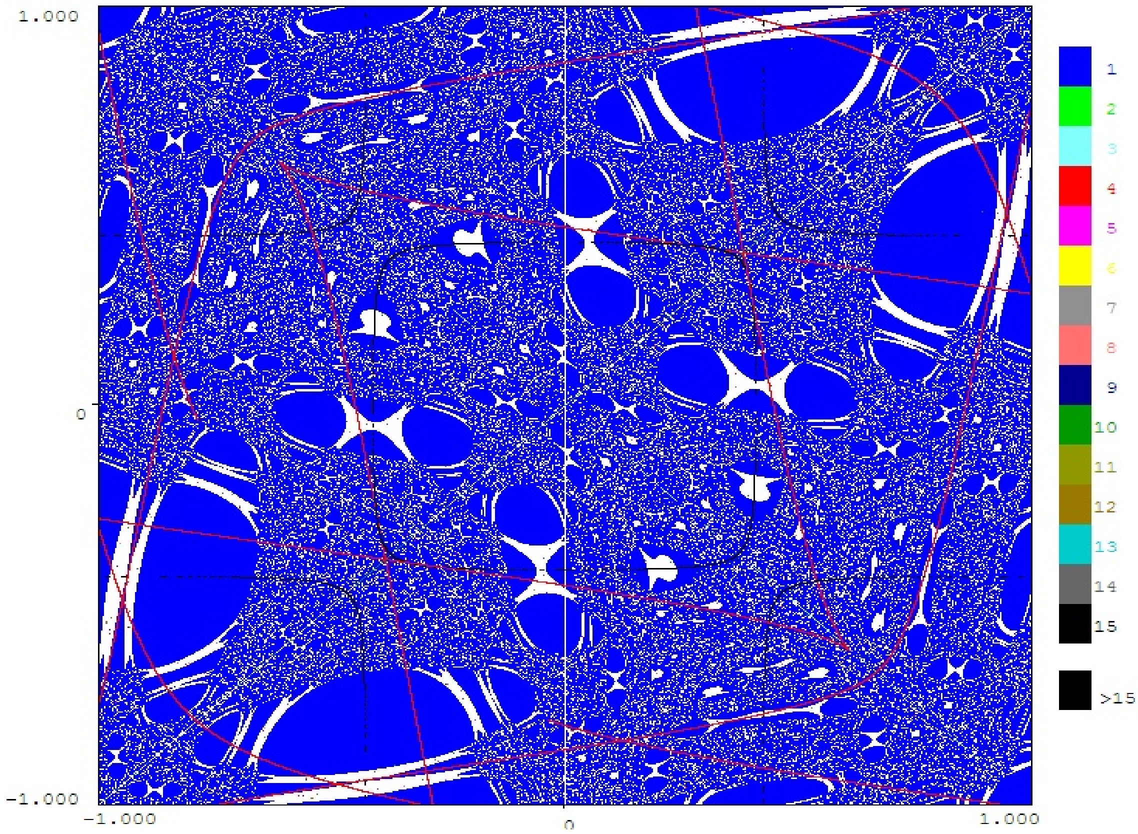

Figure 6. Fractal structures appear in the dynamical system (2), at $a = 4$ and $b = 0.6$. $B(E_1)$ is the basin of fixed points (blue color). $B(A)$ is the basin of the chaotic attractor (white color).

4. Chaotic Synchronization of the Coupled Map (2)

Because of the symmetry of map (2), the diagonal is mapped into itself, so $T(\Delta) \subseteq \Delta$. Trajectories that are embedded in Δ, i.e., $x_n = y_n$ for every n, are synchronized. If $|x_n - y_n| \rightarrow 0$ as $n \rightarrow +\infty$, a trajectory starting from Δ, with $x \neq y$, is said to synchronize [40–47], and its asymptotic behavior is defined by the simpler one-dimensional model (3). If it is a chaotic attractor for the map (3), then it is also a chaotic attractor for the two-dimensional map (2) (see [13,48]), due to the possibility of chaos synchronization.

The coupling parameter b is a normal parameter that has no effect on the dynamics along the invariant submanifold Δ. This enables us to consider a fixed value of the parameter $a = 3.11$, resulting in the existence of a chaotic attractor A of the map (3). As illustrated in Figure 7a for $b = -1$, we obtain two chaotic attractors A_1 and A_2 along the diagonal, A_1 in the region $x > 0$ and A_2 in the region $x < 0$. Thus, A_1 and A_2 are Milnor attractors, and local riddling takes place. Trajectories starting from the initial conditions in the white region of Figure 7a lead to asymptotic synchronization [49–51].

For the scenario of two coupled map (2), we observe the result displayed in Figure 7, where $a = 3.11$ and $-1 \leq b \leq -0.62$. The one-dimensional chaotic attractors A_1 or A_2 attract points from their neighborhood along the diagonal. There are also other initial conditions whose trajectories converge to another attractor, leading to the appearance of four small chaotic attractors that are created by the evolution of the local bifurcation of the asynchronous period-4 attractor. These chaotic attractors are represented by the green color in Figure 7e (zoom). The two chaotic attractors of the diagonal (see Figure 7d) are created by the evolution of the local bifurcation. For example, the attractor formed by a two-piece quasi-periodic attractor, developed by two cyclic closed invariant curves. The time development of the system is characterized by many bursts away from Δ before synchronization occurs when $b = -0.62$, and the transient is produced (see Figure 7d). This phenomenon is known as on-off intermittency.

The basins of A_1 and A_2 are globally riddled due to a boundary crisis or final bifurcation between the minimal invariant absorbing area of the synchronized chaotic attractor and the basin boundary. Therefore, the system (2) has coexisting solutions, both embedded into the invariant diagonal Δ (synchronized solutions), and out of Δ, with chaotic attractors, symmetric with respect to Δ (symmetric solutions). The creation of several coexisting chaotic attractors is characterized by basins of attraction with complicated topological structures.

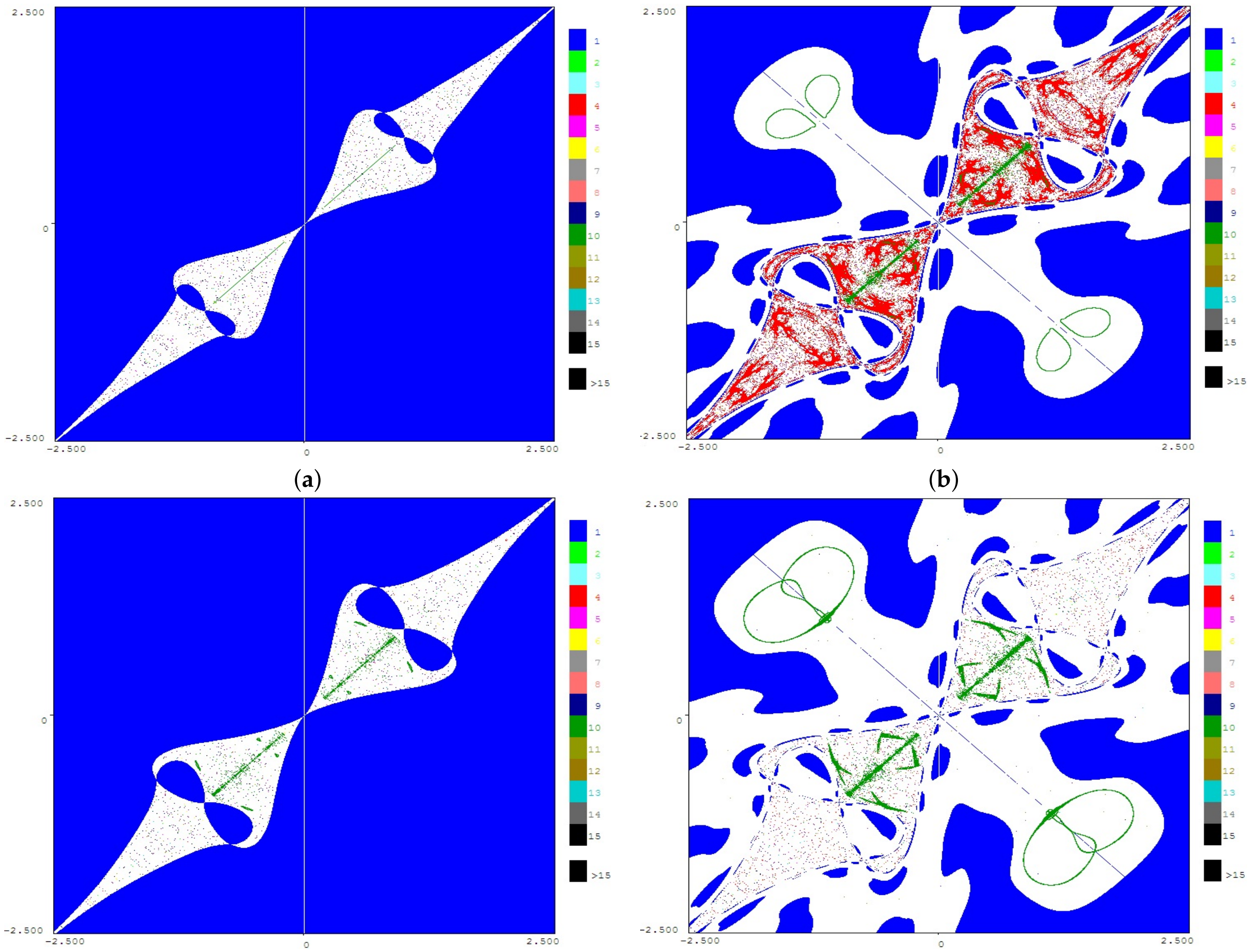

(**a**) (**b**)

(**c**) (**d**)

Figure 7. *Cont.*

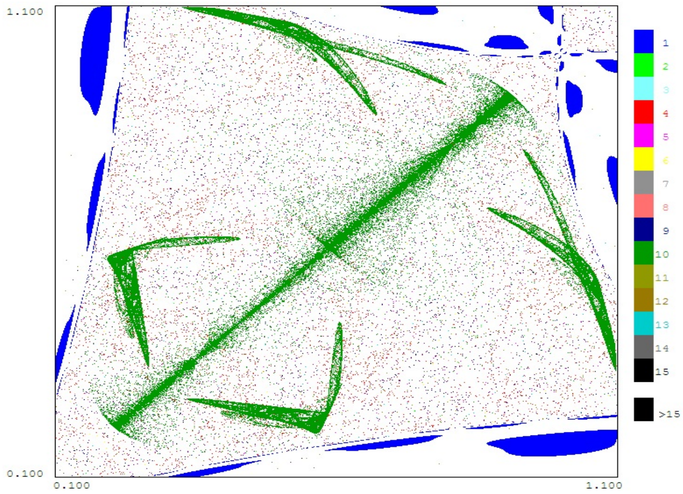

(**e**)

Figure 7. (**a**) With $b = -1$ numerical approximation of intermingled basins of attraction of an Milnor attractor A_1 in $x = y, x > 0$, other points are an approximation of the basin of Milnor attractor A_2 in $x = y, x < 0$ for the map (2). (**b**) For $b = -0.82$, a four-cyclic chaotic attractor is present (green color) that is symmetric with respect to A_1, and a four-cyclic chaotic attractor is present (green color) that is symmetric with respect to A_2. (**c**) For $b = -0.65$, the basins of the four cyclic chaotic attractor are shown in red, while in (**d**), two chaotic attractors are created by local bifurcations, developed from the asynchronous period-2 attractor. (**e**) Detail around of A_1 and a four cyclic chaotic attractor. Both images show the area (x, y) in $[-3, 3] \times [-3, 3]$.

5. Conclusions

This study presents an analysis of a new symmetric dynamical system represented by Equation (2). Our investigation involves the use of critical curves LC to explore global bifurcations that induce qualitative changes in the shape of chaotic attractors and the topological structure of basins. We present detailed images and general information on the basin structures, and we utilize geometrical and numerical methods to demonstrate how contact bifurcations can alter the character of a fractal basin. Our analysis leads us to consider critical sets and basin boundaries as the mechanism that causes complicated basins.

The strong coupling between the dual (1) or (2) maps of the system explains the inevitable presence of chaos, which also explains why coupled maps are full of riddled basins. The dynamic behavior of the system (2) is characterized by chaos synchronization and riddled basins. Moreover, coupled maps allow for more sophisticated dynamical behavior, such as the existence of one or more coexisting attractors in addition to the synchronized state. Although finite attractors are less likely to occur, the existence of an attractor at infinity is quite common. In such cases, our analysis can be extended to the characterization of global riddling.

Looking forward, we propose two future directions for our research. Firstly, we aim to investigate the foliation of the phase plane for the non-invertible map (2). The notion of foliation of the phase plane for two-dimensional non-invertible maps is essential for understanding the properties relating to maps. In our case, the critical lines LC divide the phase plane into zones noted Z_k, where $k \geq 0$. Secondly, we plan to explore the characteristics and dynamical behaviors in the space of the parameters (a, b) associated with our dynamical system (2) using both analytical and numerical methods.

In summary, this study sheds light on the properties and behaviors of the symmetric dynamical system represented by Equation (2). We believe that our findings have significant implications for understanding complex dynamical systems, and we hope that our work will inspire further research in this area.

Author Contributions: Conceptualization, Y.S., H.J., A.A.A.-B. and I.M.; Methodology, Y.S., H.J., A.A.A.-B. and I.M.; Software, Y.S., H.J., A.A.A.-B. and I.M.; Validation, Y.S., H.J., A.A.A.-B. and I.M.; Formal analysis, Y.S., H.J., A.A.A.-B. and I.M.; Investigation, Y.S., H.J., A.A.A.-B. and I.M.; Resources, Y.S., H.J., A.A.A.-B. and I.M.; Data curation, Y.S., H.J., A.A.A.-B. and I.M.; Writing—original draft, Y.S., H.J., A.A.A.-B. and I.M.; Writing—review & editing, Y.S., H.J., A.A.A.-B. and I.M.; Visualization, Y.S., H.J., A.A.A.-B. and I.M.; Supervision, Y.S., H.J., A.A.A.-B. and I.M.; Project administration, H.J., A.A.A.-B. and I.M.; Funding acquisition, Y.S., H.J., A.A.A.-B. and I.M. All authors have read and agreed to the published version of the manuscript.

Funding: This research work was funded by Institutional Fund Projects under grant no. (IFPIP: 599-611-1443). The authors gratefully acknowledge technical and financial support provided by the Ministry of Education and King Abdulaziz University, DSR, Jeddah, Saudi Arabia.

Acknowledgments: This research work was funded by Institutional Fund Projects under grant no. (IFPIP: 599-611-1443). The authors gratefully acknowledge technical and financial support provided by the Ministry of Education and King Abdulaziz University, DSR, Jeddah, Saudi Arabia.

Conflicts of Interest: The authors declare no conflict of interest.

References

1. Ding, M.; Yang, W. Observation of intermingled basins in coupled oscillators exhibiting synchronized chaos. *Phys. Rev.* **1996**, *54*, 2486–2494. [CrossRef] [PubMed]
2. Milnor, J. On the concept of attractor. *Commun. Math. Phys.* **1985**, *99*, 177–195. [CrossRef]
3. Alexander, J.C.; Yorke, J.A.; Yan, Z.; Kan, I. Riddled basins. *Int. J. Bifurc. Chaos* **1992**, *2*, 795–813. [CrossRef]
4. Maistrenko,Y.L.; Maistrenko, V.L.; Popovich, A.; Mosekilde, E. Transverse instability and riddled basins in a system of two coupled logistic maps. *Phys. Rev.* **1998**, *57*, 2713–2724. [CrossRef]
5. Maistrenko,Y.L.; Maistrenko, V.L.; Popovich, A.; Mosekilde, E. Role of the absorbing area in chaotic synchronization. *Phys. Rev.* **1998**, *80*, 1638–1641. [CrossRef]
6. Ott, E.; Sommerer, J.,C. Blowout bifurcations: the occurrence of riddled basins and on-off intermittency. *Phy. Lett. A*, **1994**, *39*, 47. [CrossRef]
7. Bischi, G.I.; Gardini, L.; Mira, C. Basin fractalizations generated by a two-dimensional family of $Z_1 - Z_3 - Z_1$ maps. *Int. J. Bifurc. Chaos* **2006**, *3*, 647–669. [CrossRef]
8. Abraham, R.; Gardini, L.; Mira, C. *Chaos in Discrete Dynamical Systems: A Visual Introduction in Two Dimensions*; Telos, the Electronic Library of Science; Springer: Cham, Switzerland, 1997.
9. Tramontana, F.; Gardini, L. Revisiting Samuelson's models, linear and nonlinear, stability conditions and oscillating dynamics. *J. Econ. Struct.* **2021**. 10.1186/s40008-021-00239-3. [CrossRef]
10. Misiurewicz, M.; Stimac, S. Symbolic dynamics for Lozi maps. *Nonlinearity* **2016**, *29*, 3031. [CrossRef]
11. Simpson, D. Sequences of periodic solutions and infinitely many coexisting attractors in the bordercollision normal form. *Int. J. Bifurc. Chaos* **2014**, *24*, 1430018. [CrossRef]
12. Sushko, I.; Avrutin, V.; Gardini, L. Center bifurcation in the Lozi map. *Int. J. Bifurc. Chaos*, **2021**, *16* , 2130046. [CrossRef]
13. Chazottes, J.R.; Fernandez, B. *Dynamics of Coupled Map Lattices and of Related Spatially Extended Systems*; Springer: Berlin/Heidelberg, Germany, 2005.
14. Hamri, N. E.; Soula, Y. Basins and critical curves generated by a family of two-dimensional sine maps. *Electron. J. Theor. Phys. EJTP 7* **2010**, *24*, 139–150.
15. Lai, Y.C.; Grebogi, C. Noise-induced riddling in chaotic systems. *Phys. Rev. Lett.* **1996**, *77*, 5047–5050. [CrossRef]
16. Lai, Y.C.; Grebogi, C.; York, J.A. Riddling bifurcation in chaotic dynamical systems. *Phys. Rev. Lett.* **1996**, *77*, 55-58. [CrossRef] [PubMed]
17. Mira, C.; Rauzy, C. Fractal aggregation of basin is lands in two-dimensional quadratic noninvertible maps. *Int. Bifurc. Chaos* **1995**, *5*, 991–1019. [CrossRef]
18. Mira, C. *Chaotic Dynamics*; World Scientific: Singapore, 1987; p. 472. [CrossRef]
19. Mira, C.; Gardini, L.; Barugola, A.; Cathala, J.C. *Chaotic Dynamics in Two-Dimensional Noninvertible Maps*; World Scientific Series on Nonlinear Sciences, Series A; Word Scientific Publishing: Singapore, 1996; Volume 20, p. 630.
20. Mira, C.; Gracio, C. On the embedding of a (p-1)-dimensional noninvertible map into a p dimensional invertible map (p = 2, 3). *Int. J. Bifurc. Chaos* **2003**, *13*,1787–1810. [CrossRef]
21. Mira, C.; Gardini, L. *From the Box-Withinabox Bifurcation Organization to the Julia set. Part I: Revisited Properties of the Sets Generated by a Quadratic Complex Map with a Real Parameter*. Int. J. Bifurc. Chaos, World Scientific Publishing Co. Pte Ltd.: Singapore, 2009. [CrossRef]
22. Sahari, M.L.; Taha, A.K.; Randriamihamison, L. Stability and bifurcations in 2-D spatiotemporal discrete systems. *Int. J. Bifurc. Chaos* **2018**, *28*, 1830026. [CrossRef]
23. Paulo, C.R. The dynamics of a symmetric coupling of three modifined quadratic maps. *Chin. Phys. B* **2013**, *8*, 080202.

24. Li, H.; Li, K.; Chen, M.; Bao, B. Coexisting infinite orbits in an area-preserving Lozi map. *Entropy* **2020**, 22, 1119. [CrossRef]
25. Frouzakis, C.E.; Gardini, L.; Kevrekidis, I. G.; Millerioux, G.; Mir, C. On some properties of invariant sets of two-dimensional Noninvertible Maps. *Int. J. Bifurc. Chaos* **1997**, *6*, 1167–1194. [CrossRef]
26. Gardini, L.; Foroni, I.; Mir, C. On a particular foliation associated with a polynomial family of noninvertible maps of the plane. *Int. J. Bifurc. Chaos*, **2004**, *5*, 1601–1624. [CrossRef]
27. Mira, C.; Fournier-Prunaret, D.; Gardini, L.; Kawakami, H.; Cathala, J.C. Basin bifurcations of two-dimensional noninvertible maps: fractalization of basins. *Int. J. Bifurc. Chaos* **1994**, *2*, 343–381. [CrossRef]
28. Bischi, G.I.; Gardini, L.; Kopel, M. Noninvertible maps and complex basin boundaries in dynamics economic models with coexisting attractors. *Chaos Complex. Lett.* **2006**, *1*, 43–74.
29. Agiari, A.; Gardini, L.; Mira, C. On the fractal structure of basin boundaries in two-dimensional noninvertible maps. *Int. J. Bifurc. Chaos* **2003**, *7*, 1767–1785. [CrossRef]
30. Bischi, G.I.; Gardini, L.; Mira, C. Plane maps with denominator. I. Some generic properties. *Int. J. Bifurc. Chaos* **1999**, *9*, 119–153. [CrossRef]
31. Leonel, R.J.; Taha, A K.; Fournier-Prunaret, D. Big Bang Bifurcation Analysis and Allee Effect in generic growth functions. *Int. J. Bifurc. Chaos* **2016**, *6* , 1650108. [CrossRef]
32. Leonel, R. J.; Taha, A. K.; Fournier-Prunaret, D. Dynamical Analysis and Big Bang bifurcations of 1D and 2D gompertz's growth functions. *Int. J. Bifurc. Chaos* **2016**, *11* , 1630030.
33. Leonel, R.J.; Taha, A.K. Allee's Effect Bifurcation in generalized logistic maps. *Int. J. Bifurc. Chaos* **2019**, *3*, 1950039. [CrossRef]
34. Leonel, R.J.; Taha, A.K. Bifurcation structures in a 2D exponential diffeomorphismwith Allee effect. *Nonlinear Dyn.* **2019**, *95.*, 3357–3374.
35. Leonel, R.J.; Taha, A.K.; Fournier-Prunaret, D. Dynamics and bifurcations of a map of homographic Ricker type. *Nonlinear Dyn.* **2020**, *102*, 1129–1149.
36. Gardini,L.; Garijo, A.; Jarque, X. Topological properties of the immediate basins of attraction for the secant method. *Mediterr. J. Math.* **2021**, *18*, 221. [CrossRef]
37. Soula, Y.; Taha, A.K.; Fournier-Prunaret, D.; Hamri, N. Bifurcations and dynamical behaviors of 2D coupled chaotic sine maps. *Appl. Comput. Math.* **2022**, *11*, 18–30. [CrossRef]
38. Kan, I. Open sets of diffeomorphisms having two attractors, each with an everywhere dense basin. *Bull. Am. Math.* **1994**, *31*, 68–74. [CrossRef]
39. Tutueva, A.A.; Nepomuceno, E.G.; Karimov, A.I.; Andreev, V.S.; Butusov, D.N. Adaptive chaotic maps and their application to pseudo-random numbers generation. *Chaos Solitons Fractals* **2020**, *133*, 109615. [CrossRef]
40. Li, X.-F.; Leung, A.Y.T.; Jiang, J. Synchronizability and mode-locking of two scaled quadratic maps via symmetric direct-coupling. *Chaos Solitons Fractals* **2018**, *115*, 239–247. [CrossRef]
41. Asl, M.M.; Akbarabadi, S.R. Delay-dependent transitions of phase synchronization and coupling symmetry between neurons shaped by spike-timing-dependentplasticity. In *Cognitive Neurodynamics*; Springer: Berlin/Heidelberg, Germany, 2022. [CrossRef]
42. Vincent, U.E.; Njah, A.N.; Akinlade, O. Synchronization and basin bifurcations in mutually coupled oscillators. *Pramana J. Phys.* **2007**, *68*, 749–756. [CrossRef]
43. Zia, S.M.U.; Cartney, M.M.; Martinez, B.S.J.; Ali, S. A novel image encryption technique using multi-coupled map lattice system with generalized symmetric map and adaptive control parameter. *SN Comput. Sci.* **2022**, *81*. [CrossRef]
44. Djellit, I.; Soula, Y. On riddled sets and bifurcations of chaotic attractors. *Chaos Fract. Order Syst.* **2007**, *13*, 603–614.
45. Xiong, P.-Y.; Jahanshahi, H.; Alcaraz, R.; Chu, Y.-M.; Gómez-Aguilar, J.F.; Alsaadi, F.E. Spectral entropy analysis and synchronization of a multi-stable fractional-order chaotic system using a novel neural network-based chattering-free sliding mode technique. *Chaos Solitons Fractals* **2021**, *144*, 110576. [CrossRef]
46. Jahanshahi, H.; Yousefpour, A.; Munoz-Pacheco, J.M.; Kacar, S.; Pham, V.-T.; Alsaadi, F.E. A new fractional-order hyperchaotic memristor oscillator: Dynamic analysis, robust adaptive synchronization, and its application to voice encryption. *Appl. Math. Comput.* **2020**, *383*, 125310. [CrossRef]
47. Zhang, S.; Zeng, Y. A simple Jerk-like system without equilibrium: Asymmetric coexisting hidden attractors, bursting oscillation and double full Feigenbaum remerging trees. *Chaos Solitons Fractals* **2019**, *120*, 25–40. [CrossRef]
48. Zhang, S.; Wang, X.; Zeng, Z. A simple no-equilibrium chaotic system with only one signum function for generating multidirectional variable hidden attractors and its hardware implementation. *Chaos Interdiscip. J. Nonlinear Sci.* **2020**, *30*, 053129. [CrossRef]
49. Zhang, S.; Zeng, Y.; Li, Z.; Wang, M.; Zhang, X.; Chang, D. A novel simple no-equilibrium chaotic system with complex hidden dynamics. *Int. J. Dyn. Control* **2018**, *6*, 1465–1476. [CrossRef]
50. Zhang, S.; Zheng, J.; Wang, X.; Zeng, Z. Multi-scroll hidden attractor in memristive HR neuron model under electromagnetic radiation and its applications. *Chaos Interdiscip. Nonlinear Sci.* **2021**. [CrossRef]
51. Zhang, S.; Zheng, J.; Wang, X.; Zeng, Z. A novel no-equilibrium HR neuron model with hidden homogeneous extreme multistability. *Chaos Solitons Fractals* **2021**, *145*, 110761. [CrossRef]